

**Supporting information**

**Enhancing Ion Storage and Transport in  $\text{Ti}_3\text{C}_2\text{T}_z$  MXene  
via a “Sacrificial Cations” Strategy**

Xiaodan Yin †, Wei Zheng \*†, Haifeng Tang, Li Yang, Peigen Zhang \*,  
ZhengMing Sun \*

School of Materials Science and Engineering, Southeast University, Nanjing 211189,  
P. R. China.

† These authors contributed equally

E-mail: zhengwei22@seu.edu.cn (W.Z.); zhpeigen@seu.edu.cn (P.Z.);  
zmsun@seu.edu.cn (Z.M.S.)

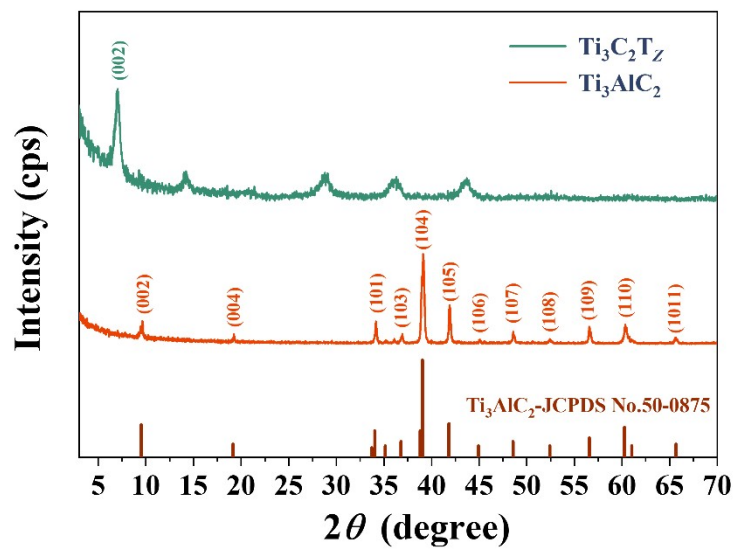


Figure S1 XRD patterns of  $\text{Ti}_3\text{C}_2\text{T}_z$  and  $\text{Ti}_3\text{AlC}_2$ .



Figure S2 The Tyndall effect of  $\text{Ti}_3\text{C}_2\text{T}_z$  suspension.

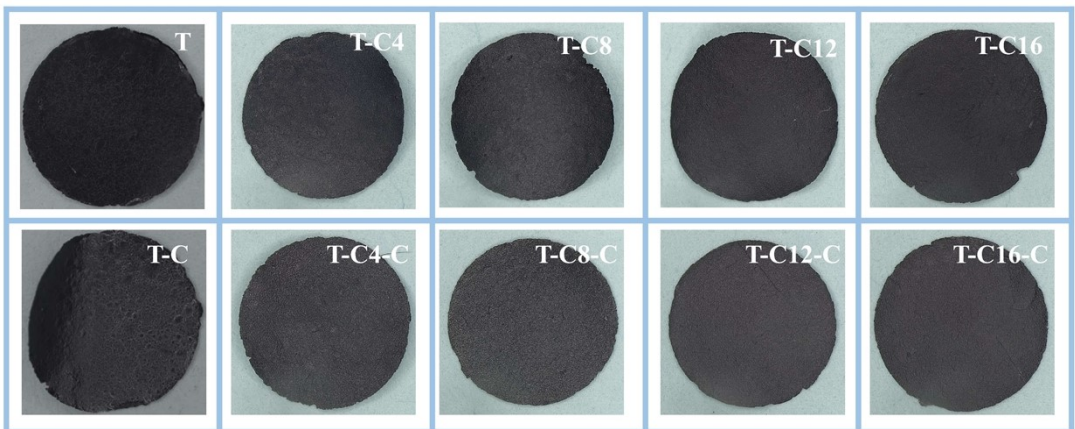


Figure S3 Optical microscope images of T, T-C, T-CX, and T-CX-C.

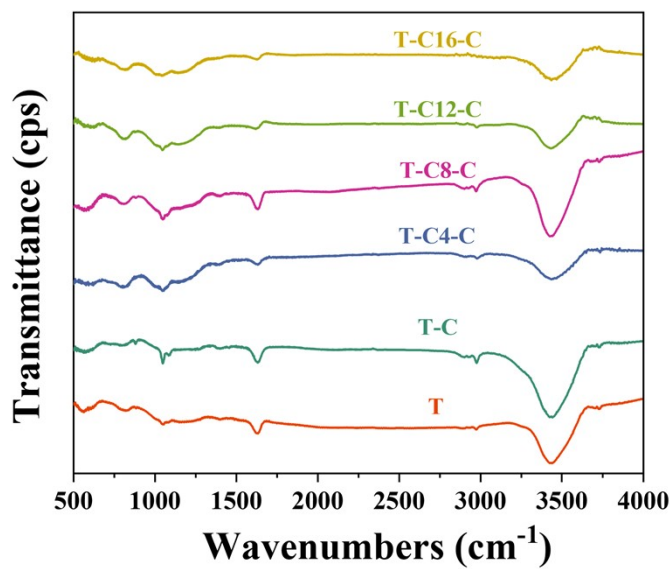


Figure S4 Fourier-transform infrared spectroscopy (FTIR) spectra of T, T-C, and T-C<sub>X</sub>-C.

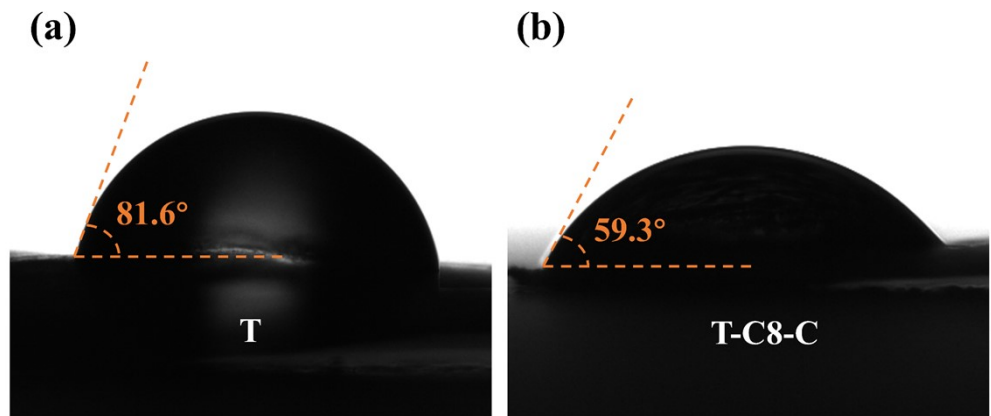


Figure S5 The contact angles of T (a) and T-C8-C (b).

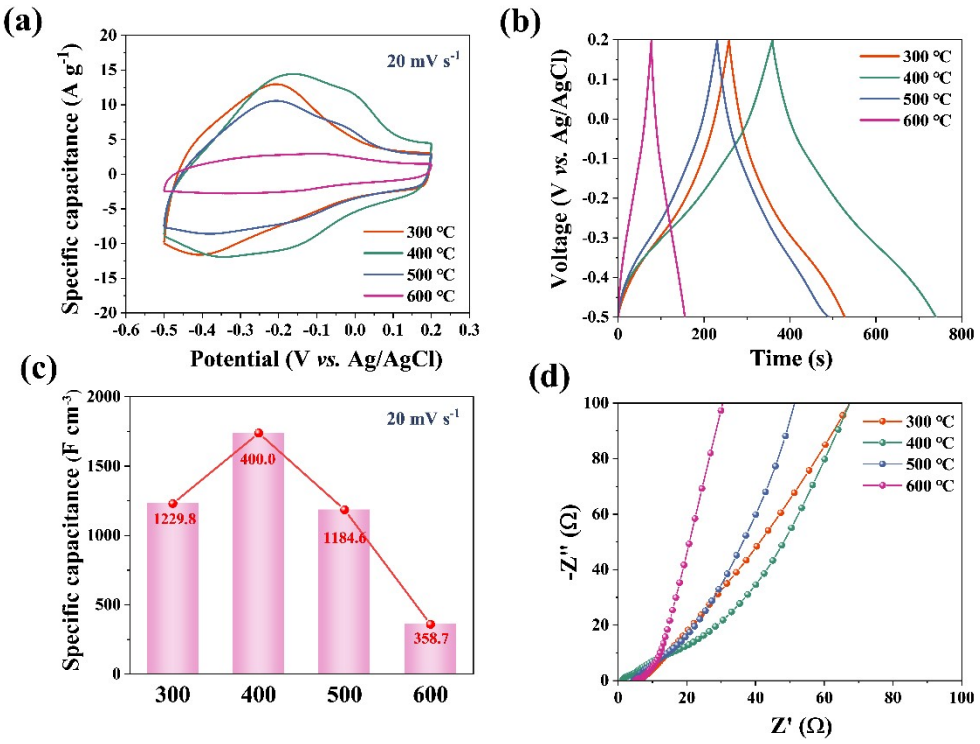


Figure S6 (a)-(b) CV and GCD curves of T-C8-C films at 300, 400, 500, and 600 °C. (c) Specific capacitances of T-C8-C films at 300, 400, 500, and 600 °C at  $20 \text{ mV s}^{-1}$ . (d) EIS curves of T-C8-C films reacted at 300, 400, 500, and 600 °C.

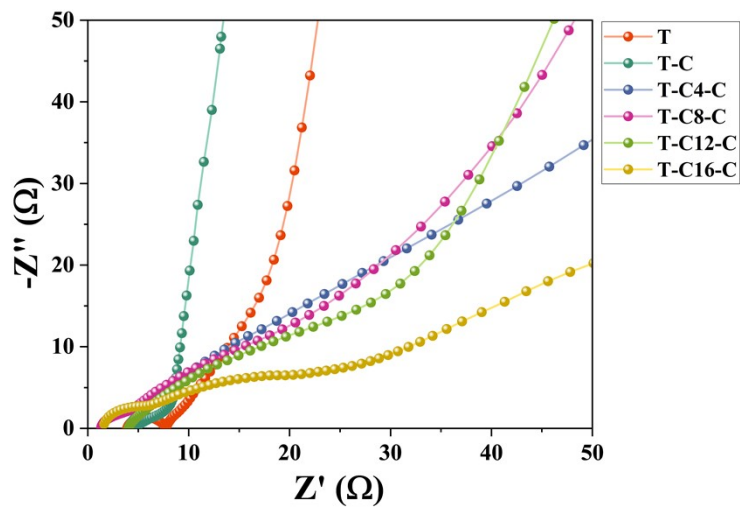


Figure S7 Nyquist plots of the T, T-C, and T-CX-C electrodes.

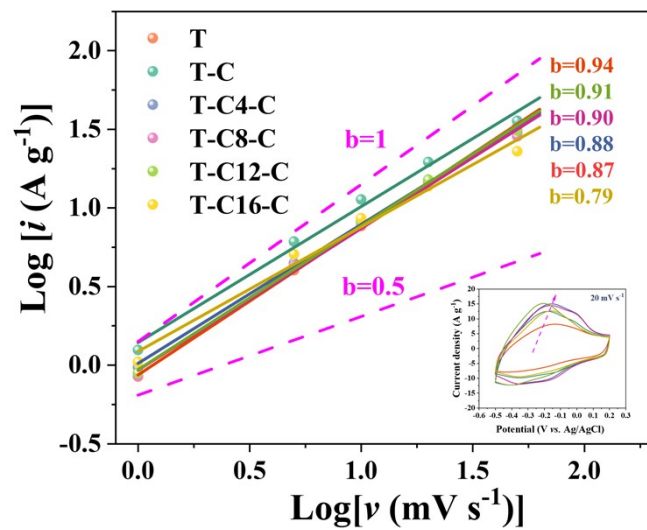


Figure S8 The  $b$  values are estimated by fitting the data for T, T-C, and T-CX-C electrodes.

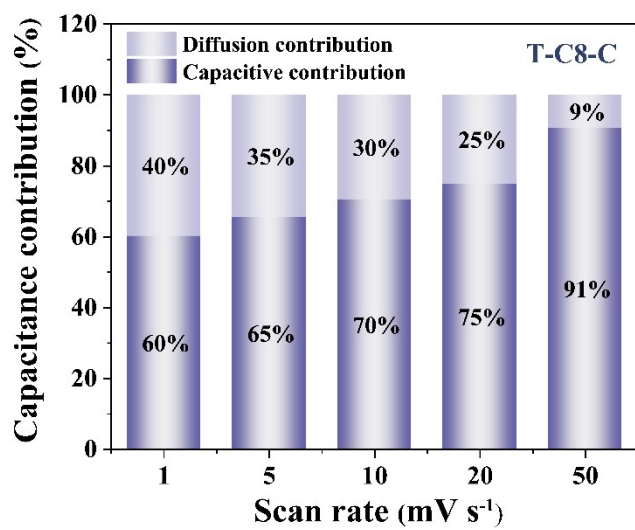


Figure S9 CV partition analysis shows the capacitive contribution to the total current at selected scan rates of T-C8-C.

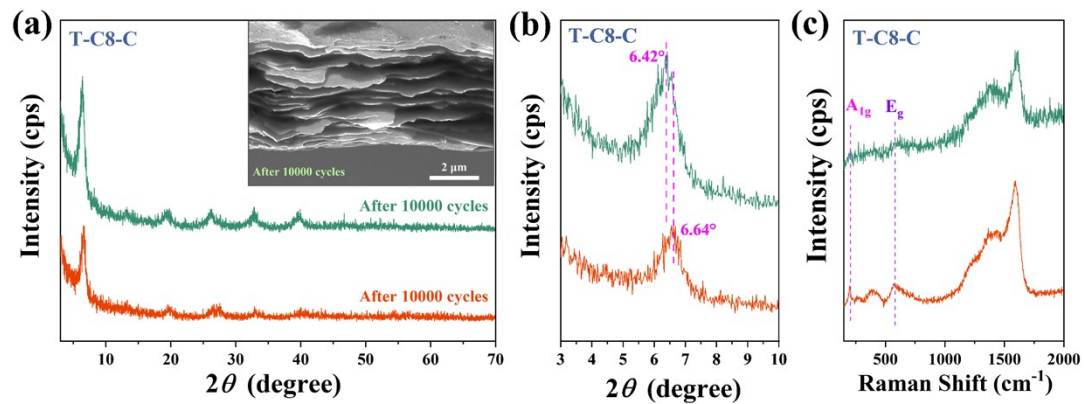


Figure S10 (a)-(b) XRD patterns of T-C8-C before and after 10000 cycles (insets show SEM image of T-C8-C after 10000 cycles) and the magnified patterns of (002) peak. (c) Raman spectra of T-C8-C before and after 10000 cycles.

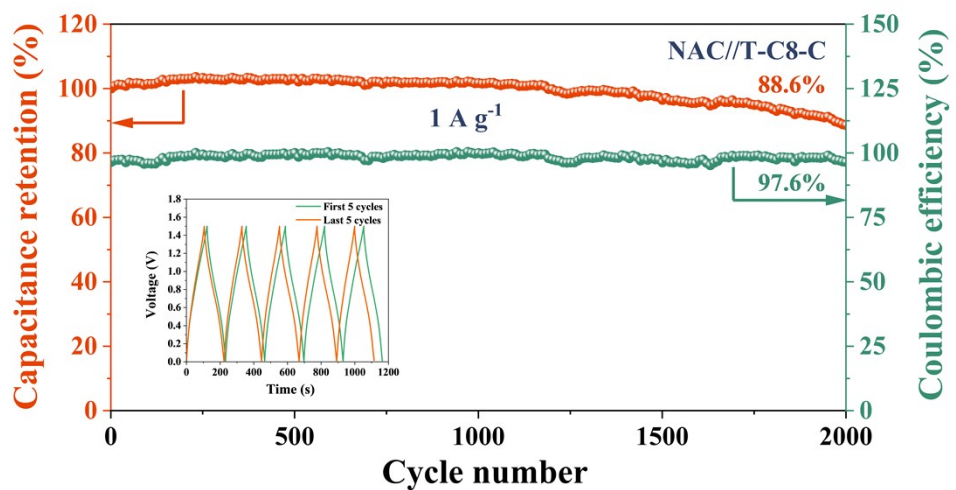


Figure S11 Cycling performance of T-C8-C//NAC at a current density  $1 \text{ A g}^{-1}$  for 2000 cycles (inset shows GCD curves of the first and last 5 cycles).

Table S1. Comparative study of MXene-based electrode materials for specific capacitance.

Electrode material	Electrolyte	Specific capacitance for single-electrode	Cycle stability	Ref
T-C8-C	3 M H <sub>2</sub> SO <sub>4</sub>	1737.6 F cm <sup>-3</sup> at 1 A g <sup>-1</sup>	102.8% for 10000 cycles	Our work
S-etched Ti <sub>3</sub> C <sub>2</sub> T <sub>x</sub> films	3 M H <sub>2</sub> SO <sub>4</sub>	1200.0 F cm <sup>-3</sup> at 5 mV s <sup>-1</sup>	99.3% for 10000 cycles	1
COF@N-Ti <sub>3</sub> C <sub>2</sub> T <sub>x</sub> /DPA	PVA/H <sub>2</sub> SO <sub>4</sub>	1298.3 F cm <sup>-3</sup> at 1 A cm <sup>-3</sup>	82.6% for 20000 cycles	2
PPy@BC/Ti <sub>3</sub> C <sub>2</sub> T <sub>x</sub>	3 M H <sub>2</sub> SO <sub>4</sub>	550.0 F g <sup>-1</sup> at 5 mV s <sup>-1</sup>	83.5% for 10000 cycles	3
MXene/AuNPs	1 M H <sub>2</sub> SO <sub>4</sub>	278.0 F g <sup>-1</sup> at 5 mV s <sup>-1</sup>	95.0% for 10000 cycles	4
Ti <sub>3</sub> C <sub>2</sub> T <sub>x</sub> -K <sub>2</sub> SO <sub>4</sub> -C	1 M H <sub>2</sub> SO <sub>4</sub>	380.0 F g <sup>-1</sup> at 2 mV s <sup>-1</sup>	90.0% for 10000 cycles	5
MXene <sub>0.9</sub>	1 M H <sub>2</sub> SO <sub>4</sub>	318.5 F g <sup>-1</sup> at 1 A g <sup>-1</sup>	92.0% for 10000 cycles	6
SNMG-40	1 M H <sub>2</sub> SO <sub>4</sub>	698.5 F cm <sup>-3</sup> at 1 A g <sup>-1</sup>	97.8% for 30000 cycles	7
Fe <sub>2</sub> O <sub>3</sub> /MXene aerogel	3 M H <sub>2</sub> SO <sub>4</sub>	182.0 F g <sup>-1</sup> at 1 A g <sup>-1</sup>	81.5 % for 10000 cycles	8
Ti <sub>3</sub> C <sub>2</sub> T <sub>x</sub> -Mn	3 M H <sub>2</sub> SO <sub>4</sub>	369.0 F g <sup>-1</sup> at 2 mV s <sup>-1</sup>	87.4% for 5000 cycles	9
Ti <sub>3</sub> C <sub>2</sub> FIBER	1 M H <sub>2</sub> SO <sub>4</sub>	309.0 F g <sup>-1</sup> at 1 A g <sup>-1</sup>	97.2% for 10000 cycles	10

## References

1. J. Tang, T. Mathis, X. W. Zhong, X. Xiao, H. Wang, M. Anayee, F. Pan, B. M. Xu and Y. Gogotsi, *ADVANCED ENERGY MATERIALS*, 2021, **11**, 2003025.
2. M. Y. Feng, Y. Zhang, X. L. Zhu, W. X. Chen, W. Y. Lu and G. Wu, *ANGEWANDTE CHEMIE-INTERNATIONAL EDITION*, 2023, e202307195.
3. Q. C. Song, Z. Y. Zhan, B. X. Chen, Z. H. Zhou and C. H. Lu, *CELLULOSE*, 2020, **27**, 7475-7488.
4. Z. X. Zheng, W. Wu, T. Yang, E. H. Wang, Z. T. Du, X. M. Hou, T. X. Liang and H. L. Wang, *JOURNAL OF ADVANCED CERAMICS*, 2021, **10**, 1061-1071.
5. Z. J. Li, J. Dai, Y. R. Li, C. L. Sun, A. L. Meng, R. F. Cheng, J. Zhao, M. M. Hu and X. H. Wang, *NANO RESEARCH*, 2022, **15**, 3213-3221.
6. J. K. Sun, Y. J. Liu, J. Y. Huang, J. T. Li, M. M. Chen, X. Y. Hu, Y. T. Liu, R. Wang, Y. A. Shen, J. J. Li, X. C. Chen, D. Qian, B. An and Z. F. Liu, *JOURNAL OF ENERGY CHEMISTRY*, 2021, **63**, 594-603.
7. L. P. Liao, D. G. Jiang, K. Zheng, M. Z. Zhang and J. Q. Liu, *ADVANCED FUNCTIONAL MATERIALS*, 2021, **31**, 2103960.
8. Y. J. Luo, Y. Tang, X. Q. Bin, C. J. Xia and W. X. Que, *SMALL*, 2022, **18**, 2204917.
9. H. J. Xu, J. X. Fan, H. Su, C. F. Liu, G. Chen, Y. Dall'Agnese and Y. Gao, *NANO LETTERS*, 2023, **23**, 283-290.
10. C. Zhu and F. X. Geng, *CARBON ENERGY*, 2021, **3**, 142-152.